

ADDIS ABABA UNIVERSITY
FACULTY OF SCIENCE
DEPARTMENT OF PHYSICS

The undersigned hereby certify that they have read and recommend to The Faculty of Science, School of Graduate Studies for acceptance a thesis entitled "*Determination of Diffusion Coefficient of Transparent Liquid Solutions using Moiré Deflectometry and On-line Monitoring of Liquid Quality by Ray Deflection*" by **Alemu Kebede** in partial fulfillment of the requirements for the degree of Master of Science in physics.

Dated; June 2006

ACKNOWLEDGEMENT

First and foremost, I thank God for everything was possible in his will. I wish to express my sincere gratitude to my advisor professor A.V Gholap for suggesting the problem of the research, his resourcefulness in forwarding instant solutions for every problem I faced especially in the construction of some apparatus from locally available materials that were important for the thesis. Moreover, his continuous follow up, motivation and his smooth but efficient communication with intra and inter-departmental and faculty bodies played the greatest role in materialization of this thesis.

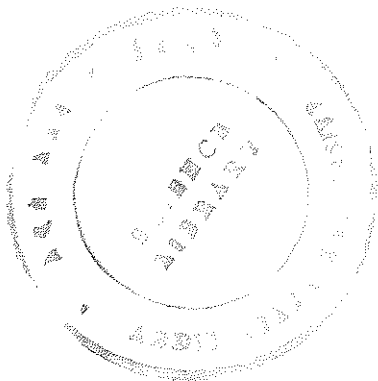
Also, I would like to thank Dr. Areaya Asfaw, Dean Faculty of Science, for facilitating the ways to get digital cameras. My thanks also goes to the following faculties, departments and persons: Faculty of Technology, department of Mechanical Engineering for their assistance in the construction of multiple slits; department of Chemistry for their assistance in the construction of diffusion tank at their glass blowing section; Geophysical Observatory for lending me their digital camera; department of Biology for lending me digital camera as well as microscope slides. My special thanks goes to Dr. Tilahun Tesfaye, Head department of Physics, for providing me with the necessary support I needed for my thesis.

Last, but not least, I would like to express my thanks to my wife W/zo Sinknesh Alemayehu and my baby son Borsuman Alemu who are always the sources of my motivation and encouragement. The care and support the whole family and friends of mine rendered me really worth acknowledging.

Abstract

In this thesis the diffusion coefficients of coffee, caffeine and sugar were investigated. The technique employed is Moiré deflectometry. New technique of on-line monitoring of the quality of liquor in the process of manufacturing is also introduced. The diffusion coefficient of caffeine was found to decrease with an increase in the caffeine concentration at constant temperature. The diffusion coefficient of grinded and sieved raw coffee at a concentration of 4.11mg/ml in distilled water, at temperature of 22°C was $(3.05 \pm 0.16) \times 10^{-6} \text{cm}^2/\text{s}$. This value of diffusion coefficient is less than the value of the diffusion coefficient of caffeine at the same concentration and temperature, in distilled water, which is $(6.13 \pm 0.16) \times 10^{-6} \text{cm}^2/\text{s}$. The main factors that are expected to have contributed to this difference are the fact that coffee is a mixture of many ingredients, as well as the particle size of the grinded raw coffee. Diffusion coefficient of 10% sugar solution in distilled water at a room temperature of 24°C was also measured and the value found is $(6.68 \pm 0.07) \times 10^{-6} \text{cm}^2/\text{s}$. On-line monitoring of a liquid quality in the process of manufacturing is also found applicable in controlling a liquid quality. This was applied to sugar solution that was made to flow through a horizontal diffusion tank and expected result was found. The qualitative aspect about any change in the index of refraction of liquid that passes through a horizontal tank with diffusion column can easily be observed by a person at work; only by referring to ray deflections that correspond to the optical density of the medium.

Key words: coffee, caffeine Moiré deflectometry, diffusion coefficient, and index of refraction



List of figures

1.1	The motion of a molecule or an atom appears to be a random walk	5
1.2	Random walk in one-dimension	8
2.1	Moiré patterns produced by two identical straight-line grating rotated by small angle from the vertical axis relative to each other.	10
2.2	Moiré between two straight-line gratings of the same pitch at an angle α With respect to one another.	12
2.3	Moiré patterns caused by two straight- line gratings with (a) the same pitch Tilted with respect to one another,(b) different frequencies and no tilt, and (c) Different frequencies tilted with respect to one another.	13
2.4	Projection of fringes or gratings on to an object and observing it an Angle α .	14
2.5	(a) maximum sensitivity for fringe projection at 90° (b) fringe produced by two interfering beams.	15
2.6	Geometry for shadow moiré where illumination and viewing points are At infinity.	16
2.7	Shadow moiré when both illumination and viewing positions are at finite distances	17
2.8	projecting moiré fringe	18
2.9	Setup for two-angle hologram	19
2.10	Shifting the angle of illumination	20
2.11	The deflection of a laser beam in a liquid of varying index of refraction	22
3.1	Experimental setup for determination of diffusion coefficients	27
3.2	Setup for on-line monitoring	28
4.1	Fringe for caffeine concentration of 4.11mg/m l	33
4.2	Fringe for caffeine concentration at 2.74 mg/ml in distilled water	35
4.3	Fringe for coffee in distilled water at a concentration Of 4.11mg/ml	34
4.4	Fringe of sugar at 10% concentration in distilled water	36

Table of contents

I. Introduction	1
1. Diffusion And Diffusion Equations	5
1.1 Diffusion Coefficient And Mean Free Path	6
1.2 Diffusion Coefficient And Viscosity	7
1.3 Random Walk As A Statistical Model For Diffusion (One-Dimensional Treatment)	7
1.4 Fickian Diffusion	8
1.4.1 Ficke's First Low	9
1.4.2 Fick's Second Law	9
2. Fringe Projection, Moiré And Moiré Deflectometry	10
2.1 Fringe Projection Techniques	14
2.2 Shadow Moiré	16
2.3 Projection Moiré	18
2.4 Two Angle Holography	19
2.5 Moiré Deflectometry	22
2.5.1 Phase Measuring Deflectometry	22
3. Experiment	27
3.1 Materials And Methods Of The Experiment	27
3.1.1 Apparatus Used	27
3.1.2 Materials Used	27
3.2 Experimental Methods And Procedures	27
3.2.1 Det Ermination Of Diffusion Coefficients Of Coffee, Caffeine And Sugar	27
3.2.2 On-Line Monitoring Of The Quality Of Liquor	29

4. Results And Discussion	31
4.1 Determination Of Diffusion Coefficient Of Caffeine	31
4.2 Diffusion Coefficient Of Grinded Row Coffee	32
4.3 Diffusion Coefficient Of Sugar In Distilled Water	35
4.4 On-Line Monitoring Of Liquids Quality	37
5. Conclusion	39
6. References	40

INTRODUCTION

Diffusion can be defined as the random walk of an ensemble of particles from regions of higher concentration to a region of lower concentration [1,17]. The process plays an important role in many fields of study in physics, chemistry, mechanical engineering etc. It helps in the study of crystal growth, pollution control, separation of isotopes, doping of impurities and also to study some biological systems [2]. Interference optical methods of observing the refractive index gradient change occurring in an initially sharp diffusing boundary has been developed to study diffusion coefficients of different kinds of fluids by Coulson, Cox, Ogsten and Philpot (1948), and Ogston (1949). They developed an apparatus called Gouy diffusiometer. It mainly served for measuring rapidly diffusing substances such as protein solutions. But the limitations of the apparatus are its sensitivity to a small temperature change and vibration [10].

The Gouy diffusiometer was applied to measuring the diffusion coefficient of caffeine in pure water. The result found showed that there was a slight decrease of the coefficient of diffusion with the increase in the concentration of the caffeine. The extrapolated graph for three data points for diffusion coefficient versus caffeine concentration at a temperature of 25^oC indicated that the value of the diffusion coefficient for caffeine at zero concentration is $6.79 \times 10^{-6} \text{ cm}^2/\text{s}$ [11].

Wave front comparison methods such as optical and holographic interferometry are among the widely used techniques for diffusivity studies. But the limitations of these techniques are their sensitivity to vibrations. Also the data has to be processed manually to obtain derivatives of the phase shift. This in turn may add to numerical errors [2]. Laser based techniques are the most sensitive methods to measure diffusion coefficient and thermal conductivity [2,3]. Their advantages are that they are non-contact methods that allow remote monitoring; show less sensitivity to vibration, have very high spatial precision, fast response time and are reliable [2, 4]. This could be possible through the development and application of the moiré fringe projection and moiré deflectometry. It begun with the careful observation of Lord Rayleigh who noticed the phenomenon of the moiré fringe in 1874. He used to look at the moiré between two identical gratings to determine their quality.

Righi (1887), first showed the relative displacement of two gratings could be determined by observing the movement of the moiré fringes.

The next significant advance in the use of moiré was presented by Weller and Shepherd (1948). They used moiré to measure the deformation of an object under applied stress by looking at the difference in grating pattern before and after the applied stress. They were the first to use shadow moiré, where a grating is placed in front of a non-flat surface to determine the shape of the object behind it by using the shape of the moiré fringe. A rigorous theory of moiré fringe did not exist until the mid fifties when Ligtenberg (1955) and Guild (1956,1960) explained moiré for stress analysis by mapping slope contour and displacement measurement, respectively. In 1967 Rowel and Welford used fringe projection technique to determine surface topography. The technique entails projecting a fringe or grating on an object and viewing it from different directions [9].

The technique was used by Brooks and Helfinger (1969) for optical gauging and deformation measurement. Until 1970, advances in moiré techniques were primarily in stress analysis. Some of the first uses of moiré to measure surface topography were reported by Meadow et al. (1970), Takasaki (1970), and Wasowski (1970).

A theoretical review and experimental comparison of moiré and projection technique for contouring is given by Benoit et al.(1975). Automatic computer fringe analysis of moiré pattern by finding fringe centers were reported by Ytagai et al. (1982). Among these techniques the moirés deflectometry is vital for the study of diffusivity of miscible fluids flow. The molecular diffusion coefficient of the fluids can be determined using physical relations between changes in the optical path length and phase properties as a function of concentration and time at a constant temperature [2,5]. The technique is applied to measuring the diffusion coefficient of a transparent liquid solution of sugar in pure water. Accordingly, the diffusion coefficient of sugar in pure water at room temperature and 10 % concentration was found to be $0.66 \times 10^{-5} \text{ cm}^2/\text{s}$. [2].

Moiré fringe projection and moiré deflectometry are among the active areas of study in recent time. Among these areas of research are: Ray deflection approach to optical testing for diagnosis of phase object and specular surface of optical devices[6], the measurement of modulation transfer function of Electra-optical system and their components such as X-ray imaging intensifier tube and fluorescence screen [7],

visualizing flow field in a diesel combustion chamber and determination of temperature distribution of its flow field quantitatively, turbulent flow of gas and temperature distribution of flame [8], and the moiré deflectometric technique for measuring the diffusion coefficient of a transparent liquid solution which was introduced in 2004 by group of researchers Kazem Jamshidi-Ghaleh, Mohammad Taghi Tavassoly and Nastaran Mansour[2]. Experimental simplicity, real-time monitoring, and less sensitivity of the moiré deflectometry to vibration makes it very suitable for application in industrial areas in addition to its reproducibility [2]. In my thesis, therefore, I will try to utilize these advantages of the technique and check whether it can be applied to controlling the quality of liquid in the process of manufacturing.

Objectives:

I. General Objectives:

The main objectives of this thesis are to determine the diffusion coefficient of transparent liquid solutions of caffeine, coffee and sugar in pure water using moiré deflectometry. Secondly, the economical utility of the technique in controlling the quality of liquor at the time of manufacturing is checked, an appropriate design of apparatus required are designed, produced from locally available materials and used for the experiment. This experiment is also aimed at assisting the country's effort in the line with quality control of some of its domestic and imported industrial items and forwarding cost and time effective alternative methods to do this. Thus, on-line monitoring of a liquid quality is introduced.

II. Specific Objectives:

The specific objectives of the experiment are to measure the diffusion coefficient of caffeine and sugar at different concentrations and time at constant temperature. The moiré fringe shifts due to ray deflection is measured for the different concentrations and analysis is made to determine the diffusion coefficient of their solutions in distilled water. Diffusion cell and an apparatus for on-line monitoring for quality control of liquid in the process of manufacturing are made from locally available materials. On-line monitoring of liquid quality by ray deflection is checked.

The thesis is presented in five chapters. The first chapter discusses about diffusion phenomena and diffusion equations such as Fick's law. It also discusses Einstein-Smoluchwsky equation and factors that affect diffusion coefficient of solute in a solvent. chapter two is about moiré fringes, fringe projection, shadow moiré and moiré deflectometry. It discusses the similarities and differences between these techniques and their areas of application. The third chapter describes the experiment; the procedures followed, materials and methods used are presented. Results and discussion on the results of the experiment are presented in unit four. Comparison between the theoretical values and the experimental results is made. Finally, conclusions and recommendations are made in the fifth chapter.



CHAPTER ONE

1. Diffusion and Diffusion Equations

Diffusion is a physical process by which matter spreads out from a region of higher concentration to a region of lower concentration. In more general terms, diffusion may refer not only to the movement of matter but also of heat. For example, if one end of metal block is heated rapidly and then the heat source is removed, over time the heat will diffuse through the block until temperature of the block becomes uniform. The fact that atoms and molecules are in constant motion is the basis for diffusion. Each molecule undergoes many collisions with other molecule in the gas or liquid medium in a very short period of time. Because of this the molecule appears to move in a somewhat random fashion. This is usually considered as random walk.

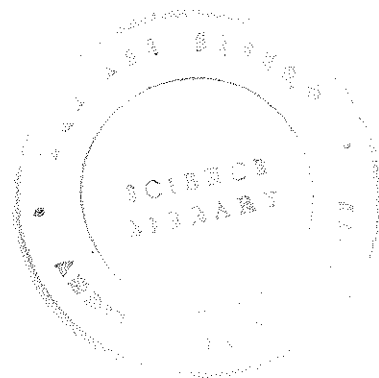
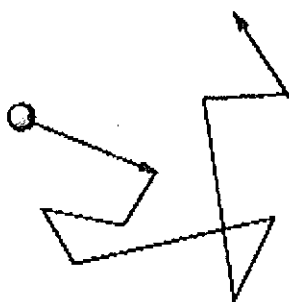


Fig.1.1 The motion of a molecule or an atom appears to be a random walk.

The average distance an atom or a molecule travels between collisions is called its mean free path. The mean free path depends upon the size of the atom or molecule. For typically small molecules such as O_2 in gas phase at 300K the mean free path is about 80nm. Taking an average speed of 400m/s the average time between collisions is about 2×10^{-10} s. This means this small molecule makes 5×10^9 collisions per second.

As the molecules undergo this seemingly random motion induced by collisions with other atoms or molecules they migrate through the solution. If there are initially larger proportions of molecules of a particular type in one region of the solution, then over time the molecules will spread out and become evenly distributed through out the solution. This is the process of diffusion. For an initial concentration gradient of a gas

or liquid media the rate at which the molecules spread out is proportional to the difference in the concentration gradient. i.e.,

$$\text{Diffusion Rate} = D \times \text{Concentration gradient} \quad (1.1)$$

Where D is diffusion coefficient in $[\text{Length}]^2 \cdot [\text{Time}]^{-1}$

It is a measure of the number of molecules moving through a particular cross-sectional area per unit of time. Experimental measurement of typical diffusion coefficient in water at 300K yields values in the range of $10^{-6} \text{cm}^2/\text{s}$.

1.1 Diffusion Coefficient and Mean Free Path

Diffusion coefficient is related to the mean free path that a molecule travels via Einstein-Smoluchowsky equation,

$$D = \frac{\lambda^2}{2\tau} \quad (1.2)$$

Where λ is the mean free path and τ is the average time between collisions.

Assuming that the average time between collisions can be calculated from the average speed and the mean free path, the time between the collisions can be expressed as,

$$\tau = \frac{\lambda}{v_{av}} \quad (1.3)$$

Where v_{av} is the average speed of the molecule.

Substituting equation (1.3) into equation (1.2) gives

$$D = \frac{\lambda v_{av}}{2} \quad (1.4)$$

Using the gas phase value of 80nm for the mean free path and 400 m / s as the average speed the predicted diffusion coefficient for a small molecule is $2 \times 10^{-5} \text{m}^2/\text{s}$; which is much larger than the typical value for the diffusion coefficient of liquid phase. i.e, $10^{-9} \text{m}^2/\text{s}$.

1.2 Diffusion Coefficients and Viscosity

Diffusion in fluid medium is related to a measurable property called viscosity. Viscosity is the measure of the resistance of the fluid to flow. Liquids such as water that flow easily have a relatively low viscosity compared to thicker fluids. The viscosity of a liquid is also its measure to transport momentum. Its unit is poise (P), where $1\text{P} = 0.1\text{kgm}^{-1}\text{s}^{-1}$. Typical viscosities are in the range of 10^{-4}P for gas and 10^{-2}P for liquids. The relationships between diffusion coefficient and viscosity is given by Einstein-Stokes equation

$$D = \frac{KT}{6\pi\eta R} \quad (1.5)$$

Where K is Boltzman's constant T is the temperature and R is the radius of the molecule. The equation is derived, of course, assuming that the molecule is spherical in shape. Qualitatively the Einstein-Stokes equation shows that viscosity and diffusion coefficient are inversely related. D is also related to temperature via the equation

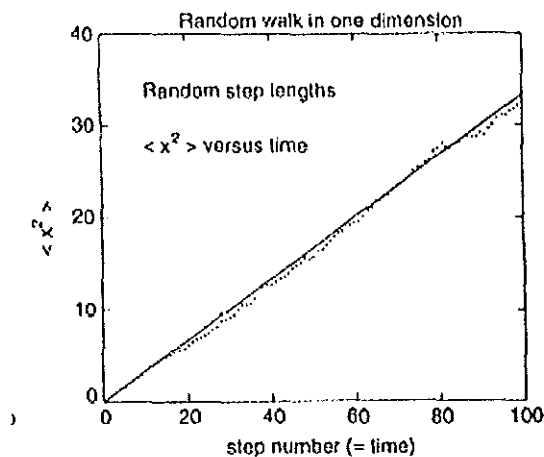
$$D = D_0 \exp(-E_A/RT) \quad (1.6)$$

Where D_0 is diffusion coefficient at infinite temperature (maximum diffusion coefficient) and E_A is activation energy.

1.3 Random Walk as a Statistical Model for Diffusion (One-Dimensional Treatment)

Processes such as diffusion in which a single molecule moves through a solution a huge number of other particles, can be modeled statistically. Even though the presence of other particles can affect the dynamics of the particle of interest through collision and interactions we can consider the motion of the particle as a random walk. The simplest example of this type of modeling is one-dimensional random walk. The diffusion motion of random walk simulation can be shown by calculating the average square distance from the origin, $\langle x^2 \rangle$. To do this, many individual random walk simulations are carried out, and the average is taken over many individual random walks.

Results for $\langle x^2 \rangle$ versus time for a random walk in one dimension is shown in fig.1 2. below.



Results for $\langle x^2 \rangle$ versus time for random walk in one dimension (from *Computational Physics*, N. J. Giordano, Prentice Hall, Upper Saddle River, NJ, 1997).

Fig.1.2 Diffusion and random walk

The result presented in the figure shows that the system follows the equation

$$\langle x^2 \rangle \propto D t \quad (1.7)$$

Where t is the time (proportional to the number of steps) and D is the diffusion coefficient.

1.4 Fickian Diffusion

In 1885, Adolf Fick introduced two differential equations that quantify the inter diffusion between two species in which there is no net volume change across the plane of reference. If one species is large and dictates a low diffusion rate for the system, one diffusion equation can be used to describe the phenomena.

1.4.1 Ficke's First Law:

It states that the flux J of a component of concentration C , across a membrane of area in a predefined plane, is proportional to the concentration differential across that plane. i.e.

$$J = -D\nabla C \quad (1.8)$$

Where J is the particle flux, C is the concentration of the solute, D is the diffusion coefficient, ∇ (del) is the differential vector operator and is represented by

$$\nabla = \frac{\partial}{\partial x} \vec{i} + \frac{\partial}{\partial y} \vec{j} + \frac{\partial}{\partial z} \vec{k} \quad (1.9)$$

Accordingly,

$$J = -D \left(\frac{\partial}{\partial x} C\vec{i} + \frac{\partial}{\partial y} C\vec{j} + \frac{\partial}{\partial z} C\vec{k} \right) \quad (1.10)$$

For one-dimensional expansion equation (1.10) reduces to,

$$J = -D \left(\frac{\partial}{\partial x} C \right) \quad (1.11)$$

The negative sign shows that diffusion takes place in the direction of decreasing concentration

1.4.2 Fick's Second Law:

It states that the time rate of change of concentration in a volume element of a membrane with in the differential field is proportional to the rate of change of flux gradient at that point in the field. i.e.

$$\frac{\partial C}{\partial t} = -\nabla J \quad (1.12)$$

CHAPTER TWO

2. Fringe Projections, Moiré and Moiré Deflectometry

The term moiré is a French word, which refers to an irregular wavy finish, usually produced on a fabric by pressing between engraved rollers (Webster's 1981). In optics it refers to a beat pattern produced between two gratings of approximately equal spacing. Lord Rayleigh used moiré for reduced sensitivity testing for the first time in 1874. He looked at the moiré between two identical gratings to determine their quality even though each individual grating could not be resolved under a microscope.

Fringe projection entails projecting a fringe or grating pattern on an object and viewing it from different directions. Rowe and Welford presented the first use of fringe projection for determining surface topography in 1967. It is a convenient technique for contouring objects that are too coarse to be measured with a standard interferometry.

Moiré and fringe projection interferometry compliment the conventional holographic interferometry, especially for testing optics to be used at longer wavelengths. It can contour surfaces at any wavelength longer than 10-100 μm with reduced environmental requirements and no intermediate photographic recording setup. Moiré is also a useful technique for aiding in the understanding of interferometry and interferometric results.

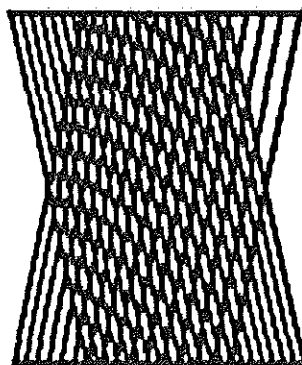


Fig.2.1 moiré patterns produced by two identical straight line grating rotated by small angle from the vertical axis relative to each other.

Dark fringes are produced when the lines are out of phase by one-half period and bright fringes are produced when the dark line of one grating fall on top of the corresponding dark line for the second grating. If the angle between the two gratings is increased the separation between the bright and dark fringes decreases.

The following analysis shows how to treat moiré fringe patterns for arbitrary gratings. Let the intensity transmission functions for two gratings be $f_1(x, y)$ and $f_2(x, y)$ be given by

$$f_1(x, y) = a_1 + \sum_{n=1}^{\infty} b_{1n} \cos[n\phi_1(x, y)] \quad f_2(x, y) = a_2 + \sum_{m=1}^{\infty} b_{2m} \cos[m\phi_2(x, y)] \quad (2.1)$$

Where $\phi(x, y)$ is the function describing the basic shape of the grating lines. For the fundamental frequency $\phi(x, y)$ is equal to integer number times 2π

$$\text{i.e. } \phi(x, y) = (n 2\pi) \quad (2.2)$$

at the center of each bright line, where n is an integer.

And is equal to an integer plus one-half times 2π at the center of each dark line,

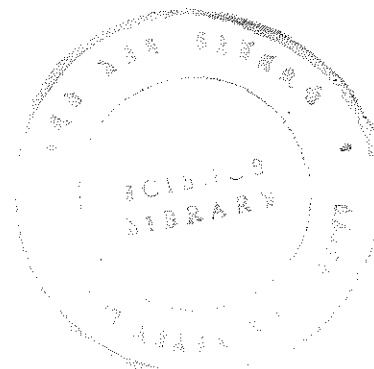
$$\text{i.e. } \phi(x, y) = 2\pi (n+1/2) \quad (2.3)$$

at the center of each dark line, where n is an integer.

The b terms determine the profile of the grating lines (i.e. square waves, sinusoidal waves, etc.). For sinusoidal waves line profile b_{11} is the only non-zero term. When these two gratings are superimposed the resulting intensity transmissions function becomes the product of the two transmission functions. i.e.

$$f_1(x, y) \cdot f_2(x, y) = a_1 a_2 + a_1 \sum_{m=1}^{\infty} b_{2m} \cos[m\phi_2(x, y)] + a_2 \sum_{n=1}^{\infty} b_{1n} \cos[n\phi_1(x, y)] + \sum_{m=1}^{\infty} \sum_{n=1}^{\infty} b_{1n} b_{2m} \cos[n\phi_1(x, y)] \cos[m\phi_2(x, y)] \quad (2.4)$$

The first three of equation (2.4) provide information that can be gained by inferring to the two gratings separately; but the fourth term contains information about the relationships between the two grating functions. Let us now express the last term as follows



$$\begin{aligned}
& \sum_{m=1}^{\infty} \sum_{n=1}^{\infty} b_{1n} b_{2m} \cos[n\phi_1(x, y)] \cos[m\phi_2(x, y)] = \frac{1}{2} b_{11} b_{21} \cos[\phi_1(x, y) - \phi_2(x, y)] \\
& + \frac{1}{2} b_{11} b_{21} \cos[\phi_1(x, y) + \phi_2(x, y)] + \frac{1}{2} \sum_{m=1}^{\infty} \sum_{n=1}^{\infty} b_{1n} b_{2m} \cos[n\phi_1(x, y) - m\phi_2(x, y)] \\
& + \frac{1}{2} \sum_{m=1}^{\infty} \sum_{n=1}^{\infty} b_{1n} b_{2m} \cos[n\phi_1(x, y) + m\phi_2(x, y)] \quad (2.5)
\end{aligned}$$

Consider the first term of equation (2.5) above: It represents the difference between the fundamental patterns masking up the two gratings. Also, assume that the two gratings are oriented at an angle 2α between them with the Y-axis of the co-ordinate system bisecting this angle as shown in the fig. below.

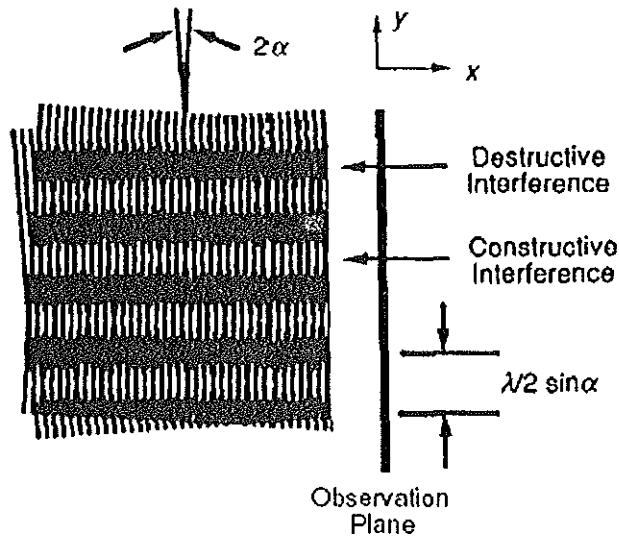


Fig.2.2 Moiré between two straight-line gratings of the same pitch at an angle 2α with respect to one another.

Then the two grating functions can be written as,

$$\phi_1(x, y) = \frac{2\pi}{\lambda_1} (x \cos \alpha + y \sin \alpha) \text{ and } \phi_2(x, y) = \frac{2\pi}{\lambda_2} (x \cos \alpha - y \sin \alpha) \quad (2.6)$$

Where λ_1 and λ_2 are the line spacing of the two gratings. Taking the difference between the two grating functions in equation (2.6) we have

$$\phi_1(x, y) - \phi_2(x, y) = \frac{2\pi}{\lambda_{beat}} x \cos \alpha + \frac{2\pi}{\lambda} y \sin \alpha \quad (2.7)$$

Where $\bar{\lambda} = \frac{\lambda_1 \lambda_2}{\lambda_1 + \lambda_2}$ the average in line spacing and $\lambda_{beat} = \frac{\lambda_1 \lambda_2}{\lambda_2 - \lambda_1}$ is the beat wavelength between the two gratings. The moiré or beat will be the lines whose center satisfies the equation

$$\phi_1(x, y) - \phi_2(x, y) = 2\pi m \quad (2.8)$$

Where m is an integer that correspond to the fringe order. Now we can consider three different cases.

I. When $\lambda_1 = \lambda_2 = \lambda$

In this case the first term in equation (2.7) has to be zero so that the equation becomes meaningful. Thus the fringe center is given by

$$\begin{aligned} \phi_1(x, y) - \phi_2(x, y) &= \frac{2\pi}{\lambda} y \sin \alpha = 2\pi m \\ \Rightarrow m \lambda &= 2y \sin \alpha \end{aligned} \quad (2.9)$$

As it is expected this is an equation of an equi-spaced horizontal lines.

II. Let the fringes be parallel to each other with $\alpha = 0^\circ$,

This makes the second term of (2.7) vanish. The moiré will then become lines that satisfy the condition

$$m \lambda_{beat} = x \quad (2.10)$$

Fig.2.3 shows the moiré patterns caused by two straight-line gratings under 3 conditions.

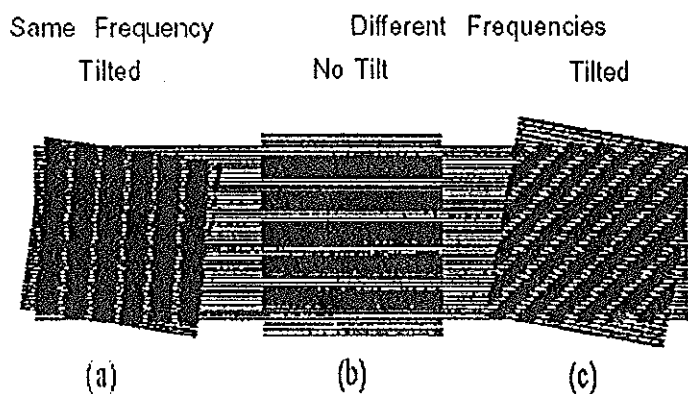


Fig.2.3 moiré patterns caused by two straight- line gratings with (a) the same pitch tilted with respect to one another,(b)different frequencies and no tilt, and (c)different frequencies tilted with respect to one another.

III. When the two gratings have different line spacing and the angle between them is non-zero, In this case the equation for the moiré fringe will be

$$m \bar{\lambda} = \frac{\bar{\lambda}}{\lambda_{beat}} x \cos \alpha + y \sin \alpha \quad (2.11)$$

Equation (2.11) represents straight-line fringes whose spacing and orientation depends on the relative difference between the spacing of the two gratings and the angle between them.

2.1 Fringe Projection Techniques

A simple approach to contouring is to project interference fringes of gratings on to an object and viewing it from different directions

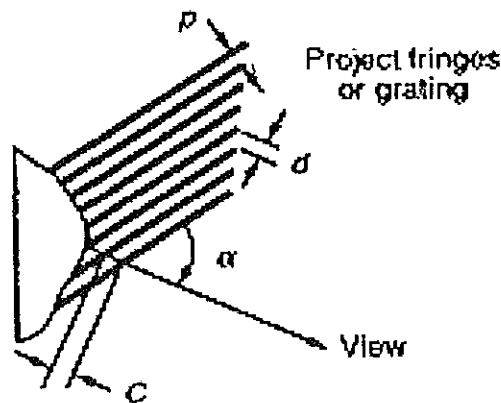


Fig.2. 4 projection of fringes or gratings on to an object and observing it an angle α . P is the periodicity of the gratings (pitch) and C is the contour interval.

Assuming a collimated illumination of beam and viewing the fringes with telecentric optical system, straight, equally spaced fringes that are incident on the object produces equally spaced contour intervals. Any departure of a viewed fringe from a straight line shows the departure of the surface from a plane of reference. When the

$$C = \frac{p}{\sin \alpha} = \frac{d}{\tan \alpha} \quad (2.13)$$

These contour lines are planes of equal heights; and the sensitivity of the measurement is determined by α . The larger the α , the smaller the contour interval. If α is 90° the sensitivity is maximum; the reference plane will be parallel to the direction of the fringes and perpendicular to the viewing direction as shown in fig.5,(a) below. When α is zero the contour intervals will be infinite and the measured sensitivity is zero. For best results an angle no longer than the largest slope on the surface should be chosen.

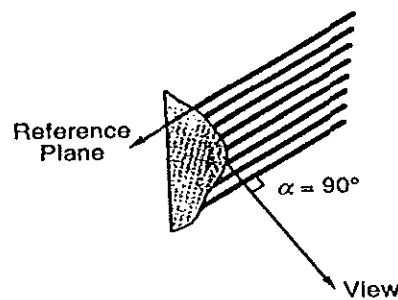


Fig.2.5 (a) maximum sensitivity for fringe projection at 90°

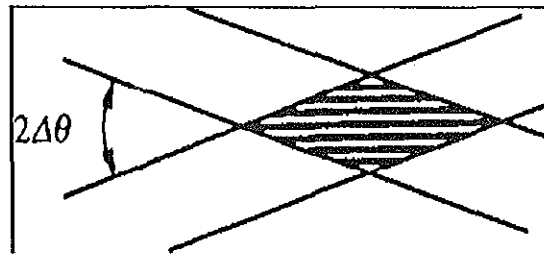


Fig.2.5 (b) fringe produced by two interfering beams.

When interference fringes are projected onto a surface rather than using a grating the fringe spacing P is determined by the relation

$$P = \frac{\lambda}{2 \sin \Delta\theta} \quad (2.14)$$

When λ is the wavelength of illumination and $\Delta\theta$ is the angle between the two interfering beams. Substituting the value of P into (2.14) the contour interval becomes,

$$C = \frac{\lambda}{2 \sin \Delta\theta \sin \alpha} \quad (2.15)$$

Tilting one beam with respect to the other will change the contour interval; the larger the angle between the two beams the smaller the contour interval will be. If the source and the viewer are not at infinity, the fringes or gratings projected onto the object will not be composed of straight, equally spaced lines. The height between the contour planes will be a function of the distance from the source and viewer to the object.

2.2 Shadow Moiré

This is a simple method of moiré interferometry for contouring objects. It uses a single grating placed in front of the object as shown in the figure below.

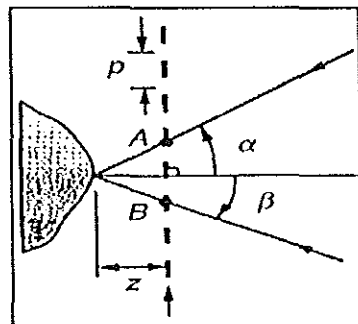


Fig.2.6 geometry for shadow moiré where illumination and viewing points are at infinity

The grating in front of the object produces a shadow on the object that is viewed from a different direction through the grating. A low frequency or pattern is seen. This is caused by the interference between the gratings shadows on the object and the grating as viewed. If we assume that the illumination is collimated and that the object is viewed at infinity or telecentric optical system is used, the height Z between the grating and the object point can be determined from the geometry shown.

$$Z = \frac{NP}{\tan \alpha + \tan \beta} \quad (2.16)$$

α is the illumination angle, β is the viewing angle, P is the spacing of the grating lines, N is the number of grating lines between the points A and B. The contour interval in the direction perpendicular to the grating will simply be given by

$$C = \frac{P}{\tan \alpha + \tan \beta} \quad (2.17)$$

As it can easily be understood from equation (2.17) the distance between the moiré fringes in the beat pattern depends on the angle between the illumination and viewing direction. The larger the angle, the smaller the contour interval; the reference plane will be parallel to the grating. Note that this reference plane is tilted with respect to the reference plane obtained if viewed projected on to the subject. Essentially the shadow moiré technique provides a way of removing the tilt term and repositioning the reference plane. Most of the time it is difficult to illuminate an entire object with a collimated beam therefore it is important to consider the case of finite illumination and viewing distances. However the only cases where illumination and viewing positions are the same distances from the grating will be used. The grating is assumed to be close enough to the object surface so that diffraction effects are negligible. The following figure illustrates this phenomenon.

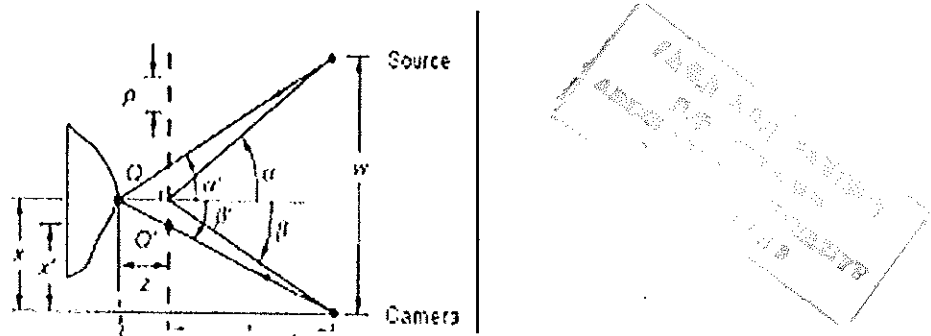


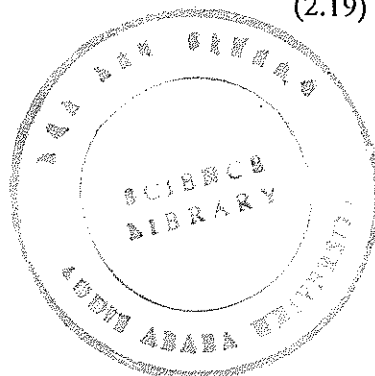
Fig.2.7 shadow moiré when both illumination and viewing positions are at finite distances.

The height between the object and the grating is given by

$$Z = \frac{NP}{\tan \alpha' + \tan \beta'} \quad (2.18)$$

α' and β' are the illumination and viewing angles at the object surface. These angles change for every point on the surface and are different from α and β , where α and β are illumination and viewing angles at the reference surface. The surface height can then be written as

$$Z = NC(Z) = \frac{NP(1+Z)}{W} = \frac{NPL}{W - NP} \quad (2.19)$$



This equation shows that the height is a complex function depending on the position of each object point. Thus the distance between the contour intervals depends on the height of the surface and the number of fringes between the gratings and the object.

Individual contour lines will no more be planes of equal heights but they are now surfaces of equal height. The expression can be simplified by considering the case where the distance to the source and the viewer is large compared to the surface variations,

i.e. $l \gg Z$. Then the surface height can be expressed as

$$Z = \frac{NPL}{W} = \frac{NP}{\tan \alpha + \tan \beta} \quad (2.20)$$

Even though the angle β and α vary from point to point on the surface, the sum of their tangents remain equal as long as $l \gg Z$ for all object points. The contour interval remains the same. Because of the finite distances there is also distortion due to the viewing perspective. A point on the surface Q appears to be at the location Q' when viewed through the grating. By similarity of triangles the distances x and x' from a line perpendicular to the grating intersecting the camera location can be related via

$$\frac{x}{z+l} = \frac{x'}{l} \quad (2.21)$$

$\Rightarrow x = x' \left(1 + \frac{z}{l}\right)$ where x represents the actual co-ordinate in terms of the measured

co-ordinates. Similarly, the y co-ordinate can be corrected as

$$y = y' \left(1 + \frac{z}{l}\right) \quad (2.23)$$

This enables the measured surface to be mapped onto the actual surface to correct the viewing perspective. These same factors can be applied to fringe projection.

2.3 Projection Moiré

Moiré interferometry can also be applied to projecting interfering fringes or grating on to an object and then viewing through a second grating in front of the viewer.

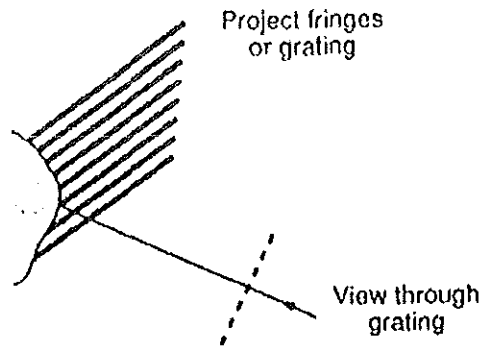


Fig.2 8 projecting moiré fringe

The difference between the projection and the shadow moiré is that two different gratings are used in the projection moiré. The orientation of the reference frame can be arbitrarily changed using different gratings pitch to view the object. The contour interval can be given by

$$C = \frac{d}{\tan \alpha + \tan \beta} \quad (2.24)$$

Where d is the period of the grating in the y plane. As long as the gratings pitches are matched to have the same value of d . This makes the projection moiré the same as shadow moiré although projection moiré can be much more complicated than the shadow moiré.

2.4 Two Angle Holography

Projected fringe contouring can also be done using holography. First the hologram of the object is made using the optical setup shown in the figure. Then the direction of the beam illuminating the object is changed slightly. When the object is viewed through the hologram then interfering fringes are seen that correspond to the interference between the wave fronts stored in the hologram and the line wave front with the tilted illumination. These fringes are illuminated simultaneously. The beams would be tilted with respect to the other by the same amount that the illumination beam was tilted after making the hologram.

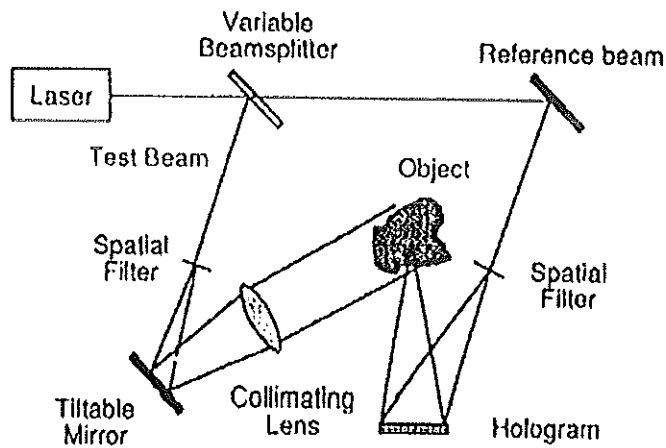


Fig.2.9 setup for two-angle hologram

To produce straight, equally spaced fringes the object illumination must be collimated. When collimated illumination is used the surface contour is measured relative to the surface that is a plane. The theory of projecting fringe contouring can be applied to two angle holography yielding a contour interval.

$$C = \frac{\lambda}{2 \sin 2\Delta\theta \sin \alpha} \quad (2.25)$$

Where $2\Delta\theta$ is the change in the angle of the object illumination.

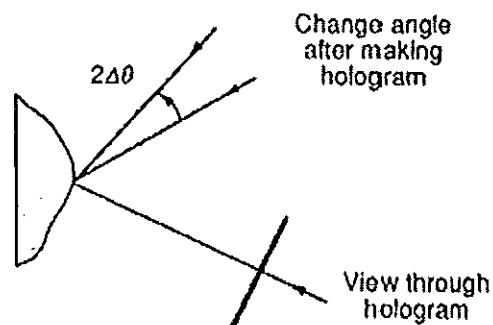


Fig.2.10 Shifting the angle of illumination

The common features of all the techniques described above produce fringes corresponding to contours of equal heights on the object. They all have a similar contour interval determined by the fringe spacing or grating period and the angle between the illumination and viewing directions as long as the illumination and viewing

are collimated. The surface height measured are relative to the reference surface that is a plane as long as the fringes or grating lines are straight and equally spaced at the object. The only difference between the fringe projection and the moiré and two-angle holography is the change in the location of the reference plane. If the fringes are digitized, or phase-measuring interferometric technique is applied the reference plane can be changed in the computer mathematically.

The precision of the interferometric technique depends on the number of fringes used. When the fringes are digitized using fringe following techniques, the surface height can be determined to 1/10 of a fringe. If phase measurement technique is used the surface height can be determined to 1/100 of a fringe. Therefore it is advantageous to use as many fringes as possible. And because reference frame can be changed in a computer, projected fringe contouring is the simplest way to contour an object interferometrically.

These techniques can all be used for measurement of stress or displacement as well as for contouring an object. Displacement measurement is made by comparing the fringe patterns obtained before and after a small movement of the object or before and after applying a load to the object. Because the sensitivity of these techniques is variable they can be used for a larger range of displacements and stress than the holographic techniques.

Using the surface measurement techniques the surface height relative to some reference surface can be obtained quantitatively. If the contour lines are straight and equally spaced in object space, then the reference surface will be a plane. In the computer, any surface described can be subtracted from the surface height to yield the surface profile relative to any surface. This is similar to viewing the contour lines through a grating to reduce their number. If the contour lines are not equally spaced and not parallel the reference surface will be something other than a plane. Therefore, surfaces are determined by placing a flat surface at the location of the object height. Once this surface is measured, it can be subtracted from subsequent measurements to yield the surface height relative to a plane surface.

2.5 Moiré Deflectometry

If a fine grid or grating is illuminated from behind through, usually, an identical grid or grating moiré fringes are produced on a screen behind the second grid or grating.

What is imaged is the composite patterns of the nearer grid or grating and the shadow on it of the grid upstream. The nearer grating is undistorted, but the distortion of the light beam (such as its divergence or convergence) lead to distortion of the shadow component and corresponding distortions in the Moiré fringes from their normally regular appearance. The distortion of the light beam could be produced by the presence of a simple lens or more interestingly phase object whose optical power varies with position in it such as a liquid with density or temperature gradients within it. Refractive index variations map onto these gradients. The refractive index variations then determine the shape of the moiré fringe.

Moiré deflectometry is a wave front technique combining Talbot effect with moiré techniques for measuring and testing phase objects or reflective surfaces. Moiré deflecograms provided by light deflection from tested phase objects or refractive surfaces can be used to calculate the deflection angle which represents the reflective index of the phase object or the height of the reflective surface. A moiré deflectometric measurement of aspheric surfaces by using digital Fourier transform method is one application area of the technique to check the evenness of a glass surface.

2.5.1 Phase Measuring Deflectometry

This is a new method of deflectometry applied to measure a specular free form surfaces within few seconds. The basic principle of the technique is to project the sinusoidal fringe patterns on to a screen located remotely from the surface under test and to observe the fringe reflected via the surface. Any slope variation leads to a distortion of the pattern. Using well known phase shifting algorithm, we can precisely measure these distortion and then calculate the surface normal in each pixel.

Moiré deflectometry is simple and powerful tool for measuring ray deflections within the paraxial approximation measurement of deflection angle of 0.1° have been reported. The main advantage of moiré defletometry are its experimental simplicity, low cost and low sensitivity to external disturbances in comparison to other interferometric methods that require high precision and stable experimental setup .

The sensitivity of the moiré deflectometry can be easily tuned to suit the experimental requirements by varying the gratings pitch and their distances (where the diffraction effects are allowed). In transparent mixture, change in concentration for a multi component liquid mixture and temperature results in a change in refractive index of the

liquid. A parallel laser beam passing through such a medium of varying index of refraction is locally deflected even if it passes perpendicular to the gradient of the diffusion direction. The deflection angle is direct mapping of the refractive index gradient of the medium.

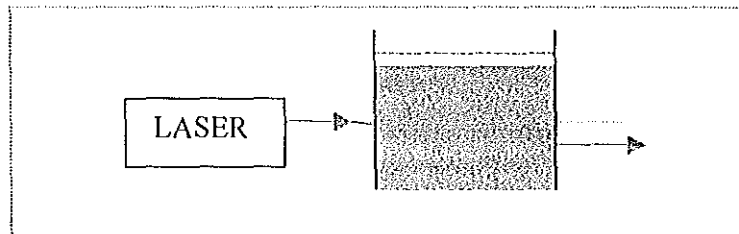


Fig.2.11 the deflection of a laser beam in a liquid of varying index of refraction



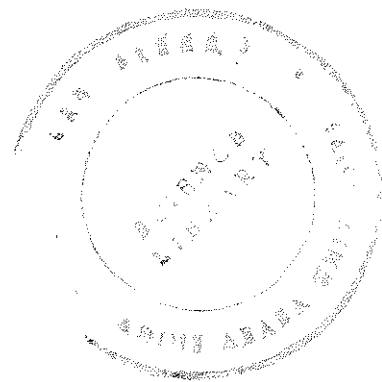
The deflected laser beam due to the change in refractive index in the diffusion cell yields the shifted self image of the gratings and resultant moiré fringes show a deviation. This can now be treated mathematically by Fick's laws of diffusion.

Let us consider the diffusion of an isothermal mixture in a container of constant cross-section, extending in the x-direction. By considering the column as semi-infinite medium, since the diffusion process is very slow, the boundary condition at the open end of the column does not influence the solution during the time range of interest. Thus the diffusion process can be formulated in terms of one-dimensional problem. One-dimensional free diffusion along the x-axis is given by the equation,

$$\frac{\partial C(x,t)}{\partial t} = D \frac{\partial^2 C(x,t)}{\partial x^2} \quad (2.26)$$

Where $C(x,t)$ is the concentration at position x and time t , and D is the diffusion coefficient which is assumed to be independent of concentration and direction of diffusion. Further more if there is a net external force F , (e.g. gravitational force), acting in the x-direction upon the dissolved molecule and if μ be the mobility of the molecule under consideration ,the steady velocity of this molecule would be μF and

the resulting flux of matter would be $C(x,t)\mu F$. The rate of concentration change would then become



$$\frac{\partial C(x,t)}{\partial t} = D \frac{\partial^2 C(x,t)}{\partial x^2} - \mu F \frac{\partial C(x,t)}{\partial x} \quad (2.27)$$

If the steady velocity of the dissolved molecules is very slow, the current due to the external forces can be neglected and equation (2.27) reduces to equation (2.26). The solution to equation (2.26) for two binary liquid mixtures initially separated at $x = 0$ when $t = 0$ with concentrations c_0 and c_1 is given by

$$c(x,t) = \frac{c_0 - c_1}{2} + \frac{c_0 + c_1}{2} \operatorname{erf} \left[\frac{x}{2\sqrt{Dt}} \right]. \quad (2.28)$$

Where the error function is defined as

$$\operatorname{erf}(x) = \frac{2}{\sqrt{\pi}} \int_0^x e^{-t^2} dt. \quad (2.29)$$

In a transparent liquid mixture, a change in concentration produces a change in the index of refraction, which for a small concentration gradient can be considered as a linear function between refraction index and concentration. The refractive index gradient is given by

$$\frac{\partial n(x,t)}{\partial x} = \frac{n_0 - n_1}{2\sqrt{\pi Dt}} \exp\left[-\frac{x^2}{4Dt}\right] \quad (2.30)$$

Where $n(x, t)$ is the local refractive index at time t in the diffusion cell, n_0 the refractive index of the liquid with higher concentration and n_1 that of the lower concentration.

The incident parallel laser beam that passes through the diffusion cell, bends by an angle $\Phi(x,t)$ depending on the distribution of the refractive index of the cell. Because the refractive index is a function of both position and time, the deflection angle also depends on position and time. Due to the deflection of the collimated laser beam, impinging on the deflectometry system, the Fourier image of the first grating shifts on the second grating. For small angle of bending light rays the amount of the image shift would be

$$\Phi(x,t) \cdot Z, \quad (2.31)$$



where
$$Z_t = \frac{mp^2}{\lambda} \dots\dots\dots (2.32)$$

Z_t is the Talbot distance between the two gratings G_1 and G_2 .

P is the periodicity of the grating; m is an integer and λ is the wavelength of the laser light. The moiré fringe shift with respect to the first grating is given by

$$\Delta\varepsilon(x,t) = \frac{z_t}{\theta} \Phi(x,t) \quad (2.33)$$

θ is a small tilt angle between the intersections of the gratings. On the other hand the relation between the integrated deflection and the local refractive index $n(x,t)$ will be,

$$\Delta\varphi(x,t) = \frac{1}{n_a} \int_0^L \left[\frac{\partial n(x,y,z,t)}{\partial x} \right]_{y=\text{const}} dz, \quad (2.34)$$

n_a is the ambient refractive index of the.

If the length of the diffusion cell in the direction of diffusion (x) is L then equation

(2.34) becomes,
$$\Phi(x,t) = \frac{L}{n_a} \frac{\partial n(x,t)}{\partial x} \quad (2.35)$$

Substituting equation (2.35) into equation (2.33) we get

$$\Delta\varepsilon(x,t) = \frac{z_t}{\theta} L \frac{\partial n(x,t)}{n_a \partial x} \quad (2.36)$$

Equation (2.36) shows that moiré fringe deformation is proportional to the refractive index gradient introduced by the diffusion process. Equation (2.36) can be modified and written as

$$\Delta\varepsilon(x,t) = \frac{z_t}{\theta} L \frac{n_o - n_1}{n_a 2\sqrt{\pi Dt}} \exp\left(\frac{-x^2}{4Dt}\right) \quad (2.37)$$

Equation (2.37) predicts the time evolution of moiré fringe along the diffusion cell. Now we can determine the diffusion coefficient at time t_o using two distinct values of position x_1 and x_2 , along the diffusion cell, where x_2 is greater than x_1 . i.e. if

$$\Delta_1 = \frac{z_t}{\theta} L \frac{n_o - n_1}{n_a 2\sqrt{\pi Dt_o}} \exp\left(\frac{-x_1^2}{4Dt_o}\right) \quad (2.38)$$

is the value of local shift at x_1 and

$$\Delta_2 = \frac{z_t}{\theta} L \frac{n_0 - n_1}{n_0 2\sqrt{\pi D t_0}} \exp\left(\frac{-x_2^2}{4D t_0}\right) \quad (2.39)$$

the local shift at x_2

Then the ratio of the local shifts is

$$\eta = \frac{\Delta_1}{\Delta_2} = \exp\left(\frac{x_2^2 - x_1^2}{4D t_0}\right) \quad (2.40)$$

Taking the logarithm of both sides we get,

$$D = \frac{x_2^2 - x_1^2}{4 t_0 \ln \eta} \quad (2.41)$$

CHAPTER THREE

3. Experiment

3.1 Materials and Methods of the Experiment

3.1.1 Apparatus

The following apparatus were used in doing the experiment: He-Ne laser source with power 1 mw and 5 mw, wave length 632.8nm, Collimator, Diffusion cell, Constricted glass tank with diffusion capillary, Sieve (250 μ m diameter), Diffraction grating with pitch 100 lines/mm, electric balance, Beakers, semitransparent screen, digital cameras and adjustable slit

3.1.2 Materials used

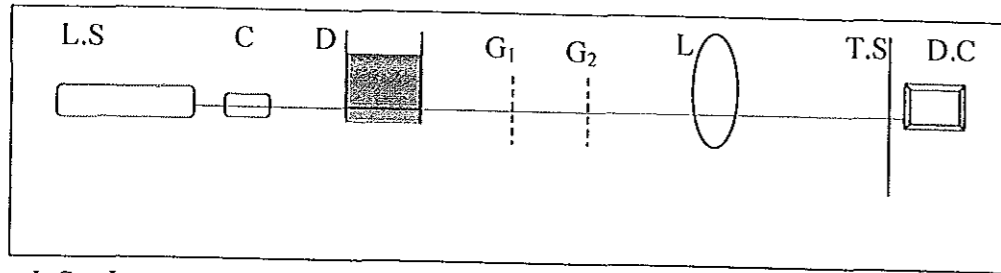
The materials used for this experiment were grinded raw coffee, caffeine and sugar.

3.2 Experimental methods and procedures

3.2.1 Determination of diffusion coefficients of coffee, caffeine and sugar

Helium-Neon laser source with wavelength of 632.8nm that can deliver a power of 1mw was sent to a collimator so that an expanded parallel light beam scans the whole column of the grating after passing through the liquid. A liquid of higher density and of the same volume was injected into the diffusion cell by a capillary tube from the bottom of the tube. The converging lens was used to converge the moiré fringe on to screen. A digital camera that has a resolving power of 2848 X 2136 pixels was used to take the image from the semitransparent screen. In order to achieve consistent results, the camera was also mounted on a stand and had been kept fixed until the experiment was over.

In the experimental analysis of sugar the digital camera used was the one with a resolution power of 640X480 pixels. In front of the diffusion cell an adjustable slit was also used to control the width of light falling on diffracting grating and hence the number and width of fringes formed when the converging lens was not used. The setup is shown in Fig. 3.1.



L.S = Laser source, C = Collimator, D= diffusion cell, G1 & G₂ = diffraction gratings,
 L= convex lens, T.S= semi-transparent screen, D.C = digital camera

Fig. 3.1 Experimental setup for determination of diffusion coefficients

After the setup shown in fig.3.1 is completed the following measurements were made:

- Choosing the right position of the Talbot distances for the gratings,
- Measuring the room temperature of the laboratory
- The diffusion coefficient of caffeine is measured for two different concentrations: 4.11 mg/ml and 2.74 mg/ml.
- Mass of coffee = 41.1mg
- The average room temperature of the laboratory was 22°C.
- Mass of the caffeine used = 41.1mg

Concentration = mass of caffeine/molar mass of caffeine x volume of the solution
 = 0.021M or

Concentration₁ = 41.1mg/10ml
 = 4.11mg/ml

Concentration₂ = 41.1mg/20ml
 = 2.74mg/ml

Distance of the screen = 62 cm

Pitch used, 100 lines /mm

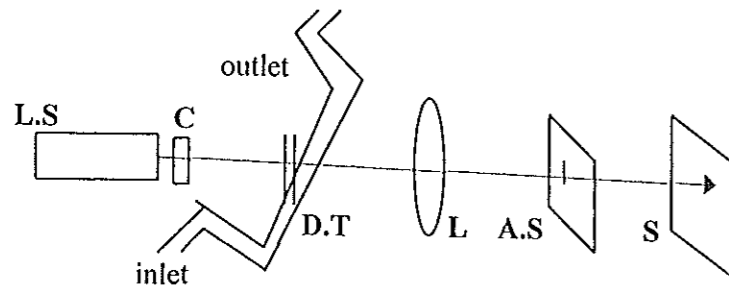
Gratings' Talbot distance = 0.8cm

Focal length of the convex lens used = 5cm

Concentration of sugar = 10%.

3.2.2 On-line monitoring of the quality of liquor^{id}

In this part of the experiment a 1mw Helium-Neon laser light scanned the column of a manometer, which is part of the horizontal diffusion tank through which liquid flows. A ray (light beam) that passes through the column of the liquid was collected by a lens and sent to an adjustable slit. The slit then throws vertical light rays onto the screen from which the shift in fringes was seen. Fig.3.2 shows the setup of the experiment. Three different concentrations of sugar solution were also used for analysis: 10%, 15% and 20%.



L.S=laser source, C = Collimator, D.T= diffusion tanker, L =lens, A.S = adjustable slit,
S = Screen

Fig. 3.2 Setup for on-line monitoring.

The following table represents the relative position of the fringe patterns for caffeine, coffee and sugar solutions as measured at the beginning of the experiment (x'_1 & x'_2) and when the fringes showed no major shift (x_1 & x_2) in the diffusion process. The calculations for local shift and diffusion coefficients were done using these values.

sample	concentration (mg/ml)	relative position in cm			
		x_2	x_1	x'_2	x'_1
caffeine	2.74	1.3	0.7	0.6	0.4
	4.11	1.3	0.8	1.2	0.6
coffee	4.11	1.3	0.6	1.1	0.5
sugar	10%	2.7	0.8	1.6	0.4

Table 3.1 Relative positions of fringes of sugar, coffee and caffeine at the given concentrations.

CHAPTER FOUR

4. Results And Discussion

4.1 Determination of diffusion coefficient of caffeine

The diffusion coefficient of a solute in a solvent depends on temperature, concentration, size of the particle and time taken for diffusion. The concentration of the solution in this experiment is also a function of position and time. The diffusion coefficient of caffeine was determined at two different concentrations. The following figures and analysis were made for these concentrations separately.

4.1.1 Caffeine concentration of 4.11 mg/ml

The following photograph was taken by a digital camera (a) at the beginning of the experiment and after 16 hour (b), when the fringes didn't show major shifts. The average room temperature was 22°C .

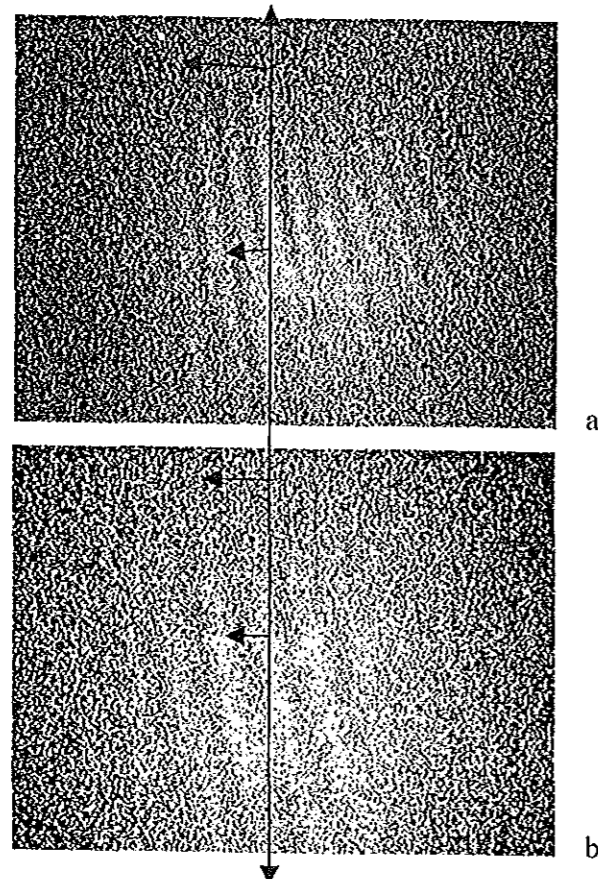


Fig.4.1 Fringe pattern for caffeine concentration of 4.11mg/m l.

For the two fringes taken at '0' and 16hr, in the figure above (a & b), the relative positions of two adjacent fringes from the vertical axis was measured. Accordingly, when $x_1 = 1.3\text{cm}$, $x_2 = 0.7\text{cm}$ for (b) and $x_1' = 0.6\text{cm}$, $x_2' = 0.4\text{cm}$ for (a), the local shifts of the fringes became,

$$\Delta_2 = 0.7\text{cm} - 0.4\text{cm}$$

$$\Delta_1 = 1.3\text{cm} - 0.6\text{cm}$$

The ratio of the two local shifts is given by

$$\eta = \frac{\Delta_1}{\Delta_2}$$

The diffusion coefficient is calculated using the equation

$$D = \frac{x_2^2 - x_1^2}{4t_0 \ln \eta}$$

The value of the diffusion coefficient $D = (0.62 \pm 0.16) \times 10^{-5} \text{cm}^2 \text{s}^{-1}$.

4.1.2 Caffeine concentration of 2.74 mg/ml

Similar procedure yields the following data for concentration of 2.74mg/ml of caffeine under similar conditions of the experiment and room temperature. The positions of the fringes were $x_1' = 1.2\text{cm}$ and $x_2' = 0.6\text{cm}$ for (c) and $x_1 = 1.3\text{cm}$ and $x_2 = 0.8\text{cm}$ for (d) where (c) and (d) refer to fringes at '0'hr. and 16hrs. respectively. (See fig.4.2). The local shifts of the fringes after 16hrs. became,

$$\Delta_2 = 1.3\text{cm} - 1.2\text{cm}$$

$$\Delta_1 = 0.8\text{cm} - 0.6\text{cm}$$

The ratios of the two local shifts will be

$$\frac{\Delta_1}{\Delta_2} = \eta$$

The diffusion coefficient is then calculated in the same way as it was done above. i.e.

$$D = \frac{x_2^2 - x_1^2}{4t_0 \ln \eta}$$

Then the diffusion coefficient is found to be $(0.66 \pm 0.16) \times 10^{-5} \text{cm}^2/\text{s}$.

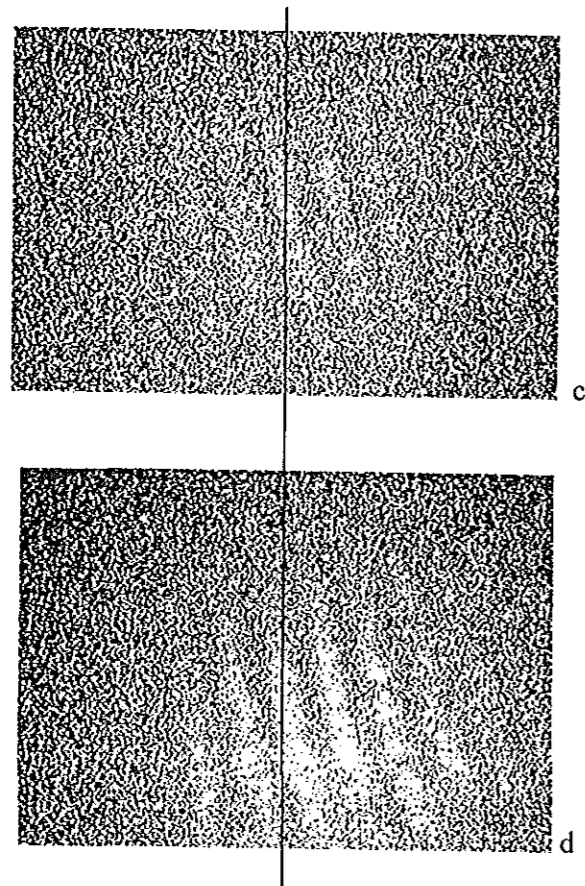


Fig. 4.2 Fringe pattern for caffeine concentration at 2.74 mg/ml in distilled water

The results for the diffusion coefficient of caffeine for the two concentrations used above show the tendency of increasing with the decrease in concentration. Moreover, the data points almost coincide with the extrapolated graph of the diffusion coefficient versus caffeine concentration found using Gouy diffusimeter in a different experiment[10].

4.2 Diffusion coefficient of grinded raw coffee

Grinded powder of raw coffee is sieved by 250 μ m diameter sieve and made to dissolve in distilled water so that it forms a solution of concentration 4.1 mg/ml similar to the first concentration of caffeine, under similar experimental condition and temperature. Figure 4.3 shows the time evolution of the fringe shifts as observed with the same digital camera. The relative positions of the fringes from the

vertical axis for '0'hr. and 16hr. is then $x_1' = 0.5\text{cm}$, $x_2' = 1.1\text{cm}$ and $x_1 = 0.6\text{cm}$ $x_2 = 1.3\text{cm}$

The value of the local shifts of the fringes after 16hr. becomes

$$\Delta_1 = 0.2\text{cm}$$

$$\Delta_2 = 0.1\text{cm}$$

Using the same relation for the ratio of the local shifts i.e.

$$\frac{\Delta_1}{\Delta_2} = \eta$$

The value of the diffusion coefficient of the raw coffee at the given concentration is then

$$D = \frac{x_2^2 - x_1^2}{4t_0 \ln \eta}$$

Thus, the diffusion coefficient becomes $(0.30 \pm 0.07) \times 10^{-5} \text{cm}^2/\text{s}$.

This value of the diffusion coefficient of coffee found is less than that of the caffeine found above. The observed decrease in the diffusion coefficient is due to: (i) the fact that coffee is a mixture that has many ingredients such as lipids and antioxidants that have different rates of diffusion. The observed diffusion coefficient is the average of all diffusion coefficients of individual particles. (ii) The other factor that is expected to be the cause for the difference is the particle size of the ground coffee. The particle size of the grinded raw coffee was $250 \mu\text{m}$ in diameter. The rate of diffusion on the other hand inversely proportional to the diameter of diffusing particles via Stokes-Einstein equation.

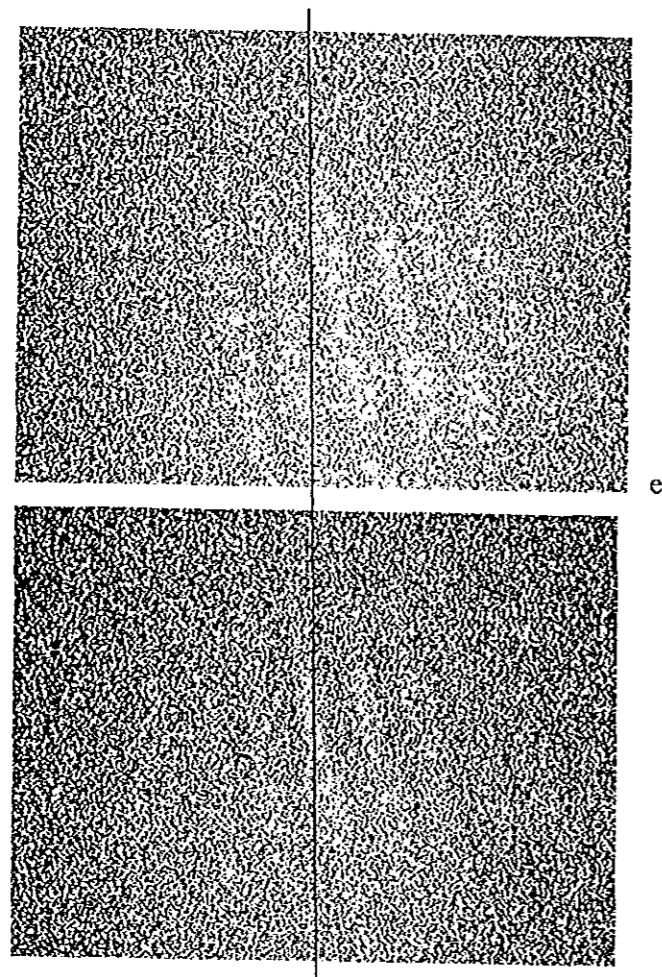


Fig.4.3 Fringe pattern for coffee in distilled water at a concentration of 4.11 mg/ml

4.3 Diffusion coefficient of sugar in distilled water

In this part of the experiment, Helium-Neon laser of power 5mw is used instead of the 1mw laser used above. This is done to check the validity of the experiment when a digital camera is used instead of the CCD camera. Also, a slit is used instead of a lens so that fringes can easily be taken from the screen behind the diffraction grating. This helps to take an image of the moiré fringes with a digital camera of less resolution power. The digital camera used in this experiment is the one with a resolution power of 640x480 pixels. The concentration of sugar used is 10%. The room temperature was 24°C. Fig. was taken at the beginning of the experiment and after 24hrs.



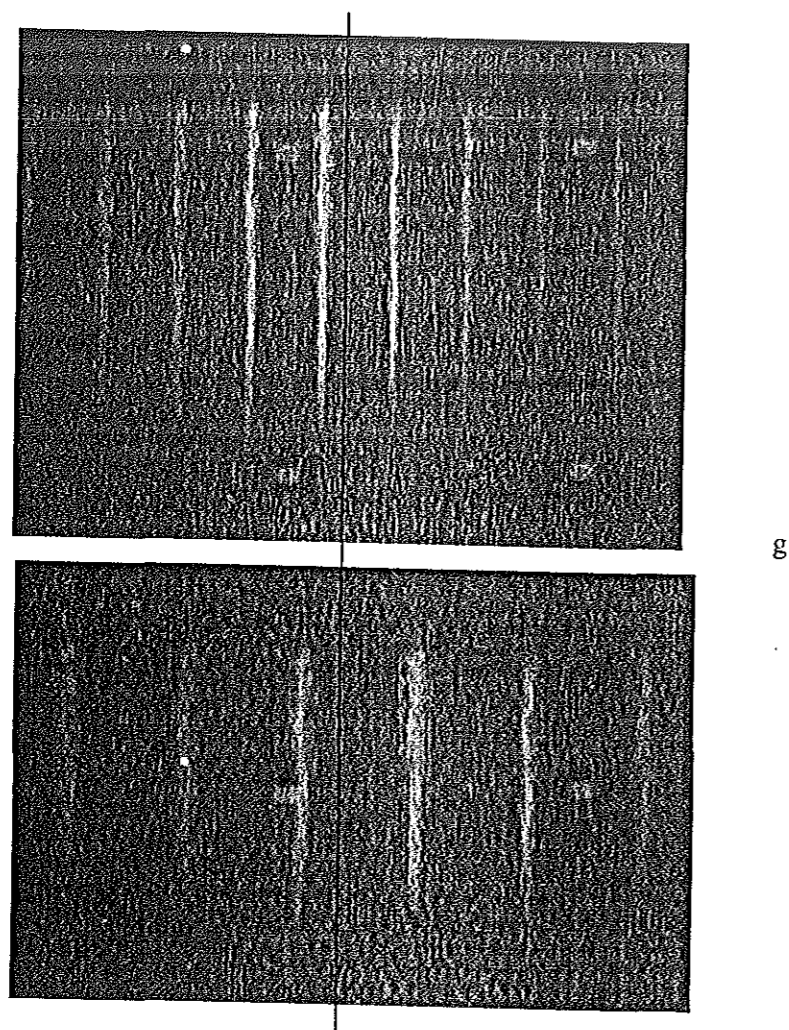


Fig.4.4 Fringe pattern of 10% sugar in distilled water

Similar formula applied to both coffee and caffeine is applied to solving the diffusion coefficient of sugar. The value found for D is given by

$$D = \frac{x_2^2 - x_1^2}{4t_0 \ln \eta}$$

The fringes didn't show major shift during the 24th hour. Thus the value of t_0 used is 86400 seconds. The value of the diffusion coefficient then became $(0.68 \pm 0.18) \times 10^{-5} \text{cm}^2/\text{s}$. The value obtained is comparable to the one found by digital holography which is $0.65 \times 10^{-5} \text{cm}^2/\text{s}$ and also by similar experiment when CCD is used $(0.66 \pm 0.05) \times 10^{-5} \text{cm}^2/\text{s}$ [2].

4.4 On-line monitoring of liquids quality

In this part of the experiment new technique to control the quality of liquid in the process of manufacturing is introduced. The setup is designed for qualitative analysis of a change in the index of refraction of a liquids in a horizontal flow that enables a practitioner or worker on duty to know whether the liquid quality is changing or not.

The experimental setup can also be applied to study the diffusion coefficient of liquids. In the experiment, the manometer column of the constricted horizontal glass container (tanker) served for two things. First, it helps for providing a flat surface that a laser light scans. Secondly, it helps for maintaining the column of the liquid in it almost at constant position so that the part of the liquid in it is not in advective or mass flow while the part of the liquid in the pipe below the column is in flow. In this experiment the deflection of a ray occurred as a liquid of different index of refraction (sugar solution) begun flowing into the horizontal pipe that contained pure water. But, the walls of the capillary tube were not perfectly flat. They had curved surfaces. This produced non-patterned and scattered fringes that were seen on a screen. To overcome this difficulty a converging lens and adjustable slit were used to cast vertical ray on to a screen. The screen was placed at 75cm away from the diffusion tank and 30cm from the slit. Also, the capillary column of the tank had to be canned so as to avoid the effect of atmospheric pressure. Moreover, flow rate had to be controlled to achieve a steady flow of the solution using rubber controller.

When sugar solution was allowed to flow through the tank, which was originally filled with tap water, a ray that was passing through the capillary part of the tank deflected from its path. Consequently ,the vertical ray that was casted on the screen shifted by 0.35 cm for 10%, 0.4cm for 15% and 0.6cm for 20% concentration of sugar solution, respectively. From this experiment it is observed that ray deflection increases with the increase in concentration. This is an expected result because an increase in concentration will increase the index of refraction of the solution, which in turn causes increase in the angle of refraction of the emergent ray [19].

Since the part of the liquid in manometer column is not in advective flow the only means by which the density or index of refraction of a liquid inside the column of the tube changed is by diffusion. The cause for the change in the index of refraction of the liquid is sugar particles that diffused into the column of the manometer. A change in the index of refraction in turn is an indication for the change in the quality of the product in the process of manufacturing.

CHAPTER FIVE

5. Conclusion

Moir'e deflectometry is a powerful tool for determining diffusion coefficient of a transparent liquid solution and also for on-line monitoring of a liquid quality in the process of manufacturing. Its experimental simplicity makes it easily adaptable to possible experimental conditions such as replacing the CCD camera by digital camera. Diffusion tank with a capillary tube in the form of a manometer made from locally available materials (glass tubes) and applied for the on-line monitoring indicated the possibility for both qualitative and quantitative analysis of liquid quality. Analysis with sugar solution showed an increase in ray deflection as the concentration of the solution that flew through the horizontal tank increased. This fact can be utilized by any practitioner at work to observe any change in the quality of his product in the process of manufacturing. If the intensity of the deflected ray is measured using CCD camera or if calculations about local shifts is made the diffusion coefficient of any transparent liquid solution can be measured quantitatively.

Investigation of the diffusion coefficient of caffeine at different concentrations in distilled water showed that it decreases with increase in concentration at constant temperature. This is in agreement with the result reported by Gosting et.al using Gouy diffusometer. On the other hand, the diffusion coefficient of a grinded raw coffee (which is a mixture of many ingredients and with larger size of grains) is found to be less than that of equal concentration of caffeine in distilled water at a given temperature showing the impact of particle size on diffusion.

In the future, the ray deflection and the moir'e deflectometric techniques have to be applied to different transparent liquid solutions so that this experimental verification of liquid quality reach a standard that can be applied to control the quality of different industrial products and imported items.

References

- [1] Paul A. Steward, Fick's Laws of Diffusion; Adapted from: Modification of the Permeability of Polymer Latex Films., Nottingham Trent University Ph.D. Thesis, (1995).
- [2] Kazem Jamshidi-Ghaleh, Mohammad Taghi-Tavassoly and Nastaran Mansour, *Diffusion coefficient Measurement of a Transparent Liquid Solution using Moir'e Deflectometry*, J.Phys. D:Appl. Phys. **37** 1993-1997 (2004).
- [3] Bindhu C.V., Harilal S.S., Nampoori V.P.N., GVallabhan C.P., *Thermal Diffusivity Measurement In Organic Liquids Using Thermal Lens Calorimetry*. Optical Engineering, **37**, 2791-2794 (1998).
- [4] Wang B., Luo X., Pfeifer T., Mischo H., *Aspheric surface measurement Using Moir'e Deflectometry based on Digital Fourier transform*. 3rd International Symposium on Test and Measurement, International Publishers. Beijing (1999).
- [5] Rashdina N, Balasubramaniam R. and Boggess M., *Concentration dependent diffusion of miscible liquids measured with interferometry*, a paper presented at the 10th International Symposium on Flow Visualization, Kyoto. Japan (2002).
- [6] Kafri O., Glatt. I., *Ray deflection approach to Optical Testing* .Optical Engineering **24**, 944-960 (1985).
- [7] Cha S., James, Trollinger D., Masaaki, Kawahashi, *Optical Techniques in fluid Thermal and Combustion Flow field*, *Journal of opt.soc.Am. A*, **2**, 107 (1985).
- [8] Scott A. Sokolofsky & Gerhard Jirka H., *Mass Transfer & Diffusion*, Institute for hydrodynamics, 2nd edition, Germany (2002).
- [9] Creath K. and Wyant J.C., *Moiré and Fringe Projection Technique* .John Wiley & Sons inc,(1992).
- [10] Creath J.M; *The use of Gouy Diffusiometer with Dilute protein Solution*, *Biochemistry* **51**, 10-17(1952).
- [11] Deshmukh A. A. *et al.*; *A precision Gouy diffusiometer*. J. Phys. E: Sci. Instrum. **3** 976-978 (1970).

- [12] Markus C., Knauer Jurgen Kaminiski and Gerd Hausler. *Phase Measuring Deflectometry*. Society of Photo-Optical Instrumentation Engineering (2004).
- [13] Schirripa G. Spagnolo and Ambarosini D. *Talbot Effect Application: Measurement of distance with Fourier Transform Method*. Meas.Sci.Technol. uk.11, 77-82(1999).
- [14] Hareesh-Tippur V. and Fu-Pen Chiang, *Analysis of combined moiré and laser speckle method used in 3-D crack tip deformation measurement*. Applied Optics 30, 2748-2756(1991).
- [15] Chon-Wen Chang, Der-Chin Su, and Jen-Tsorng Chang. *Moir'e fringes by two spiral gratings and its applications on collimation tests*. The physical Society of The Republic of China.33, 439-448 (1995).
- [16] Chien Chou and Tsu-Lung King. *Application of Moir'e phenomena. The Measurement of Modulation Transfer Function(MTF) of Electra-Optical Systems*. Chinese Journal of Physics. 19, 61-68(1981).
- [17] Steven L. Jacques, Scott A. Prahl, *Fick's laws of diffusion*; ECE532 Biomedical Optics(1998).
- [18] McCabe* M. *The diffusion coefficient of caffeine through agar gels containing a hyaluronic acid-protein complex. A model system for the study of the permeability of connective tissues*, Biochem J.; 127(1): 249-253. March (1972).
- [19] Arun Anand*, K.Vanic Chhaniwal and CS Narayana Murthy. *Diffusivity study of Transparent Liquid Solution by Imaging Beam Deflection*



DECLARATION

I hereby declare that this thesis is my original work and has not been presented for a degree in any other University. All sources of material used for the thesis have been duly acknowledged.

Name: *Alemu Kebede*
Signature:-----

This thesis has been submitted for examination with my approval as University advisor.

Name: *professor A.V Gholap*
Signature:-----

Addis Ababa University
Department of Physics
June, 2006.